

A moisture budget perspective of the amount effect

M. Moore,¹ Z. Kuang,^{1,2} and P. N. Blossey³

Received 12 October 2013; revised 27 November 2013; accepted 3 December 2013.

[1] A stable water isotopologue-enabled cloud-resolving model was used to investigate the cause of the amount effect on the seasonal (or longer) time scales. When the total water (vapor and condensed phase) budget of the precipitating column of air is considered, our results indicate that as convection becomes stronger and the precipitation rate increases, the δD of precipitation (δD_p) depends on the isotopic composition of the converged vapor more than that of surface evaporation. Tests with disabled fractionation from rain evaporation demonstrate that this mechanism does not account for the amount effect as has been previously suggested. If the isotopic content of converged vapor is made uniform with height with a value characteristic of surface evaporation, the amount effect largely disappears, further supporting the dominance of converged vapor in changes to the δD_p signal with increasing precipitation. δD_p values were compared to the water budget term $\frac{E}{P}$, where P is precipitation and E is evaporation. Results from this comparison support the overall conclusion that moisture convergence is central in determining the value of δD_p and the strength of the amount effect in steady state. **Citation:** Moore, M., Z. Kuang, and P. N. Blossey (2014), A moisture budget perspective of the amount effect, *Geophys. Res. Lett.*, 41, doi:10.1002/2013GL058302.

1. Introduction

[2] Stable water isotopologues (H_2^{16}O , HDO, H_2^{17}O , and H_2^{18}O) are useful as climate proxies and tracers of the hydrologic cycle. Slight differences in the mass of each water isotopologue changes the saturation vapor pressure of the molecule such that the heavier isotopologues tend to collect in condensed phases, while the light isotopologue accumulates in the vapor phase. This fractionation of the heavy and light molecules leads to variations in their respective ratios in a particular phase of water. Changes in these ratios can provide information about temperature [Jouzel, 2003], precipitation amount [Dansgaard, 1964; Rozanski et al., 1993], and moisture source region [Vuille et al., 2003].

[3] Isotopologue ratios in rainwater samples collected from stations included in the Global Network of Isotopes

in Precipitation [International Atomic Energy Agency/World Meteorological Organization, 2006] were analyzed by Dansgaard [1964] who noted that in the subtropics and tropics, isotopically depleted rainfall coincided with higher precipitation amounts. This relationship was termed the “amount effect” and was argued to be caused by the increased removal of heavy isotopologues by rainout as clouds cooled. This relationship was later confirmed by Rozanski et al. [1993], who repeated the analysis by Dansgaard, [1964], but with an additional 30 years of data and specifically focused on tropical marine locations.

[4] More recent studies emphasize the role of the unsaturated downdrafts that both directly and indirectly lead to isotopically depleted rainfall [e.g., Risi et al., 2008a, 2008b; Bony et al., 2008; Kurita et al., 2011]. Processes occurring in the unsaturated downdrafts that alter the isotopic composition of the falling precipitation, namely evaporation and equilibration, are referred to as direct effects. As convection strength intensifies, the precipitation rate, average drop size, and the relative humidity in the downdrafts increase. Larger drops do not evaporate as significantly as smaller drops [Stewart, 1975], and overall evaporation decreases as the relative humidity increases. Since evaporation acts to enrich the drops by preferentially removing the lighter isotopologue, decreased evaporation leads to lighter, more depleted rain and thus the amount effect [e.g., Dansgaard, 1964; Risi et al., 2008a; Bony et al., 2008].

[5] As the relative humidity increases in the unsaturated downdrafts, equilibration becomes the dominant mechanism for isotopologue exchange and acts to bring the rain and the surrounding vapor into equilibrium. When the drop size increases in strong convection, the equilibration time of the drop increases while the residence time of the drop in the boundary layer (BL) decreases, leading to rain that does not equilibrate completely with the surrounding vapor [Lee and Fung, 2008; Ciais and Jouzel, 1994; Lawrence et al., 2004; Field et al., 2010]. These partially equilibrated drops do not become as enriched as drops that reach equilibrium and instead maintain the depleted isotopic signal at the cloud base, producing the observed amount effect.

[6] The indirect influence of unsaturated downdrafts is referred to as downdraft recycling, whereby depleted vapor from the downdrafts is injected into the BL, which feeds the convective system. Downdraft vapor is depleted through efficient equilibration of the precipitation with the surrounding vapor in addition to a decreased fraction of evaporation [Risi et al., 2008a] as well as by subsidence of more depleted vapor from the environment [Risi et al., 2008a; Kurita et al., 2011; Risi et al., 2010]. The more efficient the downdraft recycling, the more depleted the precipitation that is produced by the convective system becomes.

[7] As illustrated above, much work has focused on how the boundary layer, convection, and microphysical processes conspire to produce the observed amount effect as

Additional supporting information may be found in the online version of this article.

¹Department of Earth and Planetary Sciences, Harvard University, Cambridge, Massachusetts, USA.

²School of Engineering and Applied Sciences, Harvard University, Cambridge, Massachusetts, USA.

³Atmospheric Sciences, University of Washington, Seattle, Washington, USA.

Corresponding author: M. Moore, Department of Earth and Planetary Sciences, Harvard University, Cambridge, MA 02138, USA. (moore3@fas.harvard.edu)

©2013. American Geophysical Union. All Rights Reserved. 0094-8276/14/10.1002/2013GL058302

precipitation rates increase. In contrast, *Lee et al.* [2007] and *Kurita et al.* [2009] used Global Climate Models (GCM) and found that the isotopic content of the precipitation is a consequence of moisture source region and transport patterns, which is also supported in a recent study by *Aggarwal et al.* [2012]. In this work, the authors define a residence time parameter that is implicitly dependent on both temperature and circulation patterns and find that it is positively correlated with $\delta^{18}\text{O}$ in precipitation collected from 12 global locations. A second recent study [*Kurita*, 2013] suggests that the amount effect is related to the degree of organization of convection, with relatively enriched precipitation associated with disorganized convection and more depleted precipitation arising from mesoscale convective systems.

[8] The goal of this work is to present a different interpretation as to the cause of the amount effect. In contrast to previous work that studied separate budgets of vapor and condensate [e.g., *Risi et al.*, 2008a; *Kurita*, 2013], we focus on the total column water (vapor plus condensate) budget of the precipitating column. In regions of deep convection where $P \geq E$, this budget has two sources, surface evaporation and moisture convergence, and a single sink, precipitation. We propose that the anticorrelation between the δD in precipitation (δD_p) and precipitation amount is largely a result of isotopically depleted vapor converging in the lower and middle troposphere with smaller contributions from surface evaporation. This approach is similar to that of *Lee et al.* [2007] who clearly identify the relationship between P and E and the isotopic composition of precipitation in simulations with an isotope-enabled GCM.

[9] The paper is organized so as to introduce the model and experimental setups in section 2. Model results are presented in section 3, followed by discussion of the results and the water budget terms in section 4. Finally, conclusions to this work are in section 5.

2. Model and Experiments

2.1. Model Setup

[10] The model used for this study is an isotope-enabled version of the System for Atmospheric Modeling (SAM), version 6.7 [*Khairoutdinov and Randall*, 2003] and will hereafter be referred to as IsoSAM. Isotopologue physics is implemented in the model by incorporating phase changes of the heavy water isotopologues into the Lin microphysics scheme of the Weather and Research Forecasting model, version 3.1 [*Skamarock and Klemp*, 2008]. This version of the Lin microphysics scheme closely resembles that of *Lin et al.* [1983] and is a single-moment bulk scheme that performs mixed phase saturation adjustment and does not allow for supersaturation with respect to ice at temperatures below -40°C [*Blossey et al.*, 2010]. IsoSAM incorporates the heavy isotopologues (HDO and H_2^{18}O) by replicating the transformation processes of H_2^{16}O . Fractionation is set to occur during water phase changes, which is described in detail in *Blossey et al.* [2010, Appendix B].

[11] For all of the experiments, IsoSAM is configured as a three-dimensional cloud-resolving model using a radiative-convective equilibrium (RCE) framework over an ocean surface. The simulations run for 500 days with an initial sea surface temperature (SST) of 301.15 K on a domain

that is $128 \text{ km} \times 128 \text{ km}$ with periodic boundary conditions and 64 vertical levels. The weak temperature gradient approximation (WTG) is implemented once the model reaches equilibrium, making it possible to diagnose the vertical velocity and precipitation associated with the changes in SST and prescribed temperature profiles [*Sobel and Bretherton*, 2000]. Results presented here use the damped gravity wave approach of *Kuang* [2008] and *Blossey et al.* [2009] to compute the pressure velocity perturbation. Simulations using the approach of *Sobel and Bretherton* [2000] produce similar results and will not be presented here for brevity. *Bony et al.* [2008] found using WTG to diagnose the vertical velocity in a RCE framework capable of reproducing δD_p values close to those in observations.

[12] Tendencies of moisture and temperature (represented here by χ) due to large-scale circulations that cannot be represented in our small periodic domains are calculated using equation (1):

$$\left(\frac{\partial \bar{\chi}}{\partial t}\right)_{ls} = \frac{\bar{\chi}^*}{\bar{\rho}} \frac{\partial \bar{\rho}w}{\partial z} - \frac{1}{\bar{\rho}} \frac{\partial}{\partial z}(\bar{\rho}w\bar{\chi}), \quad (1)$$

as in *Daleu et al.* [2012] and *Raymond and Zeng* [2005] (Figure S1 in supporting information for a depiction of these terms).

[13] The over bar indicates the horizontal average of the variables, and it is assumed that the horizontal wind is either into or out of the column, as represented by the upwind value χ^* . In regions of large-scale divergence ($\frac{d(\bar{\rho}w)}{dz} < 0$), the upwind value of $\chi^* = \bar{\chi}$, while in regions of large-scale convergence ($\frac{d(\bar{\rho}w)}{dz} > 0$), $\chi^* = \chi^{\text{ref}}$. The model reaches equilibrium (\sim day 60) before reference profiles are calculated (days 100–120); after which point WTG is initiated. The SST is increased by 0.5 K increments approximately every 45 days starting at day 255, providing six SST regimes ranging from 301.15 K to 303.65 K for our analysis. In all of the experiments, heavy isotopologues in the atmosphere are initialized at 0, such that the ocean is assumed to serve as an infinite source of all water isotopologues and heat.

2.2. Experimental Setup

[14] For this study, three different test cases are created to examine the different theories relating to the causes of the observed amount effect. It is first essential to see that the model is able to reproduce this relationship between the precipitation amount and the isotopic content of the precipitation. In steady state, precipitation is the sum of the surface evaporation and the horizontal convergence of moisture:

$$P = E + \left\langle \frac{q^*}{\bar{\rho}} \frac{d\bar{\rho}w}{dz} \right\rangle, \quad (2)$$

where P is the rate of precipitation and E is the evaporation. The angled brackets indicate the mass-weighted vertical integral and in cases of large-scale convergence the value of $q^* = q^{\text{ref}}$. The second term comes from equation (1) above, noting that the mass-weighted vertical integral of the second term on the right-hand side of equation (1) is zero. By using WTG, increasing SST allows for the examination of increasing precipitation regimes associated with changes in δD_p indicating the presence and strength of the amount effect. While IsoSAM is configured to simulate the microphysical processes of both HDO and H_2^{18}O , our results will be

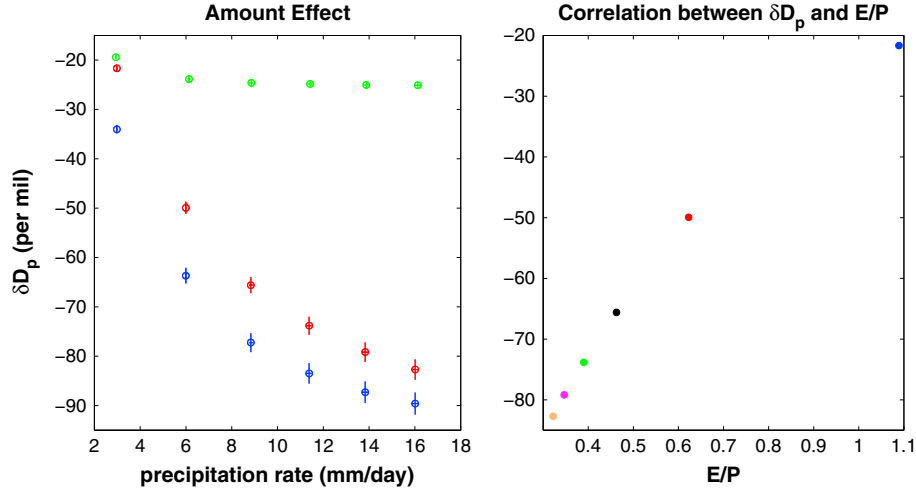


Figure 1. (left) The correlation between precipitation and δD_p for the control (red), evaporation test (blue), and uniform δD_v^{ref} profile test (green). Each of the six points per model run represent the average of the two parameters for each SST regime. The error bars in both the x and y directions indicate 1 standard deviation for precipitation rate and δD_p , respectively. (right) δD_p is compared to average values of $\frac{E}{P}$ for each SST regime (colors) of the control run.

shown in terms of HDO, since $\delta^{18}\text{O}$ and δD values are generally proportional, and showing results for both isotopologues would be redundant.

[15] Two sensitivity studies are performed to identify the key contributor to changes in δD_p with increasing precipitation. First, an evaporation test disables fractionation associated with rain evaporation and equilibration. The vapor produced by rain evaporation has the same isotopic composition as the rain itself and thus ensures that there is no preferential removal of the lighter isotopologue. This is done by setting the isotopic content of the evaporation flux to be equal to the ratio of HDO rain to H_2O rain multiplied by the amount of H_2O water evaporated from the raindrop. Prohibiting fractionation during rain evaporation can be expected to prevent the rain from becoming

increasingly heavier as the rain evaporation takes place in relatively dry air and instead should cause it to become lighter compared to the control case.

[16] Second, we performed an experiment with a reference water vapor profile that has a uniform isotopic composition with height (δD_v^{ref}). The uniform reference vapor profile is set to be -23‰ , representing the δD_v of the evaporated surface flux in the control case. As vapor generally becomes more depleted with height, using the uniform δD_v^{ref} will tend to make the isotopic composition of converged vapor and the resulting precipitation isotopically more enriched relative to the control simulation. However, in simulations where $P \sim E$ and there is no net import of vapor to the column, the effect of changing δD_v^{ref} will likely be small.

Table 1. Control Run Values and Uniform δD_v^{ref} Test Values^a

| SST | $\delta D_{\text{Sfc Evap}}$ | Evap | BL | δD_p | Prec | Conv Vap | α_{eff} |
|---|------------------------------|------------|----------------|---------------|-------------|----------------|-----------------------|
| <i>Control Run Values</i> | | | | | | | |
| 301.15 K | -25‰ | 3.1 mm/day | -93‰ | -23‰ | 3.0 mm/day | — | 1.08 |
| 301.65 K | 12‰ | 3.6 mm/day | -116‰ | -50‰ | 6.1 mm/day | -160‰ | 1.07 |
| 302.15 K | 29‰ | 4.0 mm/day | -130‰ | -66‰ | 8.9 mm/day | -152‰ | 1.07 |
| 302.65 K | 33‰ | 4.4 mm/day | -138‰ | -74‰ | 11.4 mm/day | -147‰ | 1.07 |
| 303.15 K | 35‰ | 4.8 mm/day | -143‰ | -79‰ | 14.2 mm/day | -144‰ | 1.07 |
| 303.65 K | 32‰ | 5.1 mm/day | -146‰ | -83‰ | 16.1 mm/day | -142‰ | 1.07 |
| <i>Uniform δD_v^{ref} Test Values</i> | | | | | | | |
| 301.15 K | -29‰ | 3.1 mm/day | -91‰ | -20‰ | 3.0 mm/day | — | 1.08 |
| 301.65 K | -27‰ | 3.6 mm/day | -96‰ | -25‰ | 6.1 mm/day | -21‰ | 1.08 |
| 302.15 K | -27‰ | 4.0 mm/day | -98‰ | -26‰ | 8.9 mm/day | -22‰ | 1.08 |
| 302.65 K | -29‰ | 4.4 mm/day | -98‰ | -27‰ | 11.4 mm/day | -22‰ | 1.08 |
| 303.15 K | -31‰ | 4.8 mm/day | -99‰ | -27‰ | 14.2 mm/day | -22‰ | 1.08 |
| 303.65 K | -31‰ | 5.1 mm/day | -99‰ | -28‰ | 16.1 mm/day | -22‰ | 1.08 |

^aTable includes δD_v of surface evaporation, surface evaporation rate, δD_v of boundary layer (lower 50 mb), δD_p , precipitation rate, and δD of converged vapor as well as the effective fractionation factor ($\alpha_{\text{eff}} = R_{\delta D_p}/R_{\text{BL}}$) for the control and uniform δD_v^{ref} test averaged for each SST regime. Converged vapor is near zero for the first SST regime, and thus, no δ value has been calculated.

3. Model Results

3.1. Control Case

[17] In the control run, the output produces an amount effect comparable to observations, though more depleted by as much as 40‰ for the highest precipitation rates (see Figure 1, left and Table 1). The results are also in agreement with those of previous work using a similar setup but with a single-column model [Bony *et al.*, 2008]. Since the simulation is run in RCE with an idealized representation of the large-scale circulation, one cannot expect to replicate observations exactly.

3.2. Evaporation Test

[18] Decreased rain evaporation has been argued to be a key mechanism of the amount effect [e.g., Dansgaard, 1964; Risi *et al.*, 2008a; Bony *et al.*, 2008; Lee *et al.*, 2011], and here we test this theory in our model framework by disabling fractionation during rain evaporation (i.e., vapor evaporated from rain has the same isotopic content as the rain itself).

[19] The blue points in Figure 1 (left) show the output from this experiment and due to the restriction on the rain evaporation, the rain becomes slightly more depleted than the control run. We note that the change is small between the two runs and the difference decreases as the SST increases, which is expected with increased precipitation rates and thus decreased evaporation. This leads to a smaller difference in the δD_p , while the opposite is true in lower precipitation rate cases, where rain evaporation will be greater.

[20] These small changes of δD_p values from the control run as well as the fact that the amount effect is still present indicate that rain evaporation does not appear to contribute as greatly to the amount effect as has been previously assumed. Had the evaporation been an essential part of the amount effect, disabling this fractionation process would have more of an impact on the amount effect.

3.3. Uniform δD_v^{ref} Profile Test

[21] This test demonstrates how the observed δD_p signal results from the relative contributions of the various vapor sources of distinct isotopic contents. Here the isotopic content of the environment, and thus converged vapor, is set to have the same δD value as surface evaporation. The output from this test (green points in Figure 1, left) indicates, as expected, that the amount effect essentially disappears, with δD_p values oscillating around -24‰ despite increases in the precipitation rate.

4. Discussion

4.1. Amount Effect and Moisture Convergence

[22] We present an interpretation that explains the amount effect when considering the total water (vapor plus condensate) budget of the precipitating column. Here surface evaporation and large-scale moisture convergence are the two sources of atmospheric water, and convergence of vapor is most important in determining the value of δD_p as convection strengthens. This interpretation is in accordance with Kurita [2013] who finds that an increasing fraction of stratiform (as opposed to convective) precipitation [e.g., Houze, 2004] is associated with more depleted rainfall. As the inflow to stratiform regions occurs mainly in the

midtroposphere [Mapes and Houze, 1995] where the vapor is more depleted than in the boundary layer, moisture import to these regions will reinforce the amount effect.

[23] The moisture import could potentially alter the influence of the BL vapor because of variations in the isotopic content of the converged vapor, due to changes in the structure of the vertical velocity profile. Back and Bretherton [2006] analyzed data from ERA40 and found that vertical velocity profiles in the East Pacific tend to be bottom heavy while in the West Pacific are top heavy. In the present study, the large-scale vertical velocity \bar{w} peaks in the upper troposphere for all but the coldest SST (Figure S2) so that moisture convergence occurs over a deep layer. Since the profile of δD_v becomes more depleted with height, the level of strongest convergence will influence the composition of the converged vapor; however, comparing how δD_p changes according to different vertical velocity profiles is outside the scope of this paper.

4.2. Amount Effect and Moisture Residence Time

[24] We define a budget parameter, $\frac{E}{P}$, to correlate with δD_p , similar to work by Lee *et al.* [2007]. The distinction between $\frac{E}{P}$ and residence time [Aggarwal *et al.*, 2012] is important for paleoclimate studies that use the correlation between δD_p and such parameters to estimate regional and local precipitation patterns. Held and Soden [2006] found that total precipitable water scales with the Clausius Clapeyron (CC) equation and varies by 7% per degree Kelvin change, while P (and therefore E) is much weaker than the CC scaling and only changes about 2% per degree Kelvin.

[25] The value of $1 - \frac{E}{P}$ will indicate the relative contribution of moisture convergence (and horizontal advection of upstream air into the domain, which is neglected here) in the steady state system. When $P = E$, converged vapor makes no net contribution to surface precipitation, which appears to be the case for the first SST regime (blue point in Figure 1, right). $P \gg E$ indicates that converged vapor is the primary source for precipitation. Performing the calculations with the output from the control run, we find that as the SST increases and convection becomes stronger, $\frac{E}{P}$ decreases, implying that converged vapor is making up the bulk of the precipitation.

4.3. Amount Effect and Boundary Layer Vapor

[26] Table 1 includes the δD values of the various vapor sources and the precipitation for the control run and uniform δD_v^{ref} test, respectively. Across the range of SSTs and precipitation rates in our experiments, the isotopic ratios of the boundary layer vapor and precipitation change together, with an effective fractionation factor $\alpha_{\text{eff}} = R_p/R_{\text{bl}} = 1.07 - 1.08$ that is roughly fixed and close to the equilibrium fractionation factor $\alpha_{\text{equil}} = 1.08 - 1.09$ [Majoube, 1971] at temperatures within the boundary layer. Figure S3 depicts the relationship between δD_{bl} and δD_p across the range of SSTs in our experiment. Kurita [2013] found a similar relationship in observations of the isotopic content surface vapor and precipitation, as the fit in his Figure 8 corresponds to $\alpha_{\text{eff}} = R_p/R_{\text{vap}} = 1.07 - 0.25*(R_{\text{vap}} - 0.9) \sim 1.05 - 1.08$ for the value of R_{vap} in that figure. Note that in our experiment, there is more scatter and a different slope in the relationship between R_{vap} and R_{bl} for a given SST and precipitation regime than is found across the whole range of SSTs and precipitation rates.

[27] The relative roles of post-condensation exchange, downdraft recycling, and environmental subsidence in maintaining the relationship between R_{bl} and R_p across the wide range of precipitation rates is secondary to the role of converged vapor in maintaining steady state and is thus beyond the scope of this study but is planned for future work.

5. Conclusions

[28] The goal of this study is to demonstrate that increasing convergence of water vapor is the key contributor to the observed amount effect in steady state. While a range of processes, such as entrainment, condensation, evaporation, and equilibration, are involved in producing the isotopic composition of rain, the moisture budget perspective offers a convenient overall constraint that the system must adjust to satisfy when in steady state and that offers a simple interpretation of the amount effect. We have shown that the decrease in rain evaporation and equilibration will contribute to the depletion, but the role of these processes is small compared to convergence of vapor in a steady state scenario. Results do suggest a secondary role of the boundary layer vapor, whose isotopic composition is found to be well correlated with that of precipitation across the wide range of precipitation rates in this study. However, the precise role of the boundary layer and convective processes in maintaining this relationship is outside the scope of this study.

[29] We have also proposed the parameter $\frac{E}{P}$ for comparison with δD_p . This variable indicates the strength of the hydrological cycle and provides information about the local water budget, making it possible to diagnose the relative contributions of vapor sources for precipitation in steady state. Knowing where moisture is coming from is important since a change in the moisture sources of convection could drastically alter the value of δD_p .

[30] The results presented support our hypothesis, though there are some caveats that should be addressed further in future work. As horizontal advection was neglected during our budget calculations, we intend to include this term in future work with an isotope-enabled version of the Super-Parameterized Community Atmosphere Model. Also, our results only address steady state and therefore represent the amount effect on monthly and seasonal time scales. In some instances, the amount effect has been observed on the time scale of single storms [e.g., Dansgaard, 1964; Njitchoua et al., 1999; Yoshimura et al., 2003], which the current results do not address. The arguments presented here could be applicable to individual storms, but further testing is required to confirm this.

[31] **Acknowledgments.** This research was partially supported by the Office of Biological and Environmental Research of the U.S. DOE under grant DE-SC0008679 as part of the ASR Program and NSF grants AGS-1062016, AGS-1260368, AGS-1260380 and NASA grant NNX13AN47G. The authors thank Marat Khairoutdinov for making the SAM model available. The Harvard Odyssey cluster provided much of the computing resources for this study.

[32] The Editor thanks two anonymous reviewers for their assistance in evaluating this paper.

References

Aggarwal, P. K., O. A. Alduchov, K. O. Froehlich, L. J. Araguas-Araguas, N. C. Sturchio, and N. Kurita (2012), Stable isotopes in global precipitation: A unified interpretation based on atmospheric moisture residence time, *Geophys. Res. Lett.*, *39*, L11705, doi:10.1029/2012GL015937.

Back, L. E., and C. S. Bretherton (2006), Geographic variability in the export of moist static energy and vertical motion profiles in the Tropical Pacific, *Geophys. Res. Lett.*, *33*, L17810, doi:10.1029/2006GL026672.

Blossey, P. N., C. S. Bretherton, and M. C. Wyant (2009), Subtropical low cloud response to a warmer climate in a superparameterized climate model. Part II: Column modeling with a cloud resolving model, *J. Adv. Model. Earth Syst.*, *1*(3), 14, doi:10.3894/JAMES.2009.1.8.

Blossey, P. N., Z. Kuang, and D. M. Romps (2010), Isotopic composition of water in the tropical tropopause layer in cloud-resolving simulations of an idealized tropical circulation, *J. Geophys. Res.*, *115*, D24309, doi:10.1029/2010JD014554.

Bony, S., C. Risi, and F. Vimeux (2008), Influence of convective processes on the isotopic composition ($\delta^{18}\text{O}$ and δD) of precipitation and water vapor in the tropics: 1. Radiative-convective equilibrium and Tropical Ocean-Global Atmosphere-Coupled Ocean-Atmosphere Response Experiment (TOGA-COARE), *J. Geophys. Res.*, *113*(D19), 1–21, doi:10.1029/2008JD009942.

Ciais, P., and J. Jouzel (1994), Deuterium and oxygen 18 in precipitation: Isotopic model, including mixed cloud processes, *J. Geophys. Res.*, *99*(D8), 16,793–16,803.

Daleu, C. L., S. J. Woolnough, and R. S. Plant (2012), Cloud-resolving model simulations with one and two-way couplings via the weak-temperature gradient approximation, *J. Atmos. Sci.*, *69*(12), 3683–3699.

Dansgaard, W. (1964), Stable isotopes in precipitation, *Tellus*, *16*, 436–468.

Field, R. D., D. B. A. Jones, and D. P. Brown (2010), The effects of post-condensation exchange on the isotopic composition of water in the atmosphere, *J. Geophys. Res.*, *115*, D24305, doi:10.1029/2010JD014334.

Held, I. M., and B. J. Soden (2006), Robust response of the hydrological cycle to global warming, *J. Clim.*, *19*, 5686–5699.

Houze, R. A. (2004), Mesoscale convective systems, *Rev. Geophys.*, *42*, RG4003, doi:10.1029/2004RG000150.

International Atomic Energy Agency/World Meteorological Organization (2006), Global network of isotopes in precipitation, *The GNIP Database*. [Available at <http://www.iaea.org/water/>.]

Jouzel, J. (2003), Water stable isotopes: Atmospheric composition and applications in polar ice core studies, *Treatise Geochem.*, *4*, 213–243.

Khairoutdinov, M. F., and D. A. Randall (2003), Cloud resolving modeling of the ARM summer 1997 IOP: Model formulation, results, uncertainties and sensitivities, *J. Atmos. Sci.*, *60*, 607–625.

Kuang, Z. (2008), Modeling the interaction between cumulus convection and linear gravity waves using a limited-domain cloud system-resolving model, *J. Atmos. Sci.*, *65*, 576–591.

Kurita, N., K. Ichiyanga, J. Matsumoto, M. D. Yamanaka, and T. Ohata (2009), Intraseasonal isotopic variation associated with the Madden-Julien Oscillation, *102*, *3*, 113–122.

Kurita, N., D. Noone, C. Risi, G. A. Schmidt, H. Yamada, and K. Yoneyama (2011), Intraseasonal isotopic variation associated with the Madden-Julien Oscillation, *J. Geophys. Res.*, *116*, D24101, doi:10.1029/2010JD014334.

Kurita, N. (2013), Water isotopic variability in response to mesoscale convective system over the tropical ocean, *J. Geophys. Res. Atmos.*, *118*, 10,376–10,390, doi:10.1002/jgrd.50754.

Lawrence, J. R., S. D. Gedzelman, D. Dexheimer, H.-K. Cho, G. D. Carrie, R. Gasparini, C. R. Anderson, K. P. Bowman, and M. I. Biggerstaff (2004), Stable isotopic composition of water vapor in the tropics, *J. Geophys. Res.*, *109*, D06115, doi:10.1029/2003JD004046.

Lee, J.-E., I. Fung, D. DePaolo, and C. C. Fennig (2007), Analysis of the global distribution of water isotopes using the NCAR atmospheric general circulation model, *J. Geophys. Res.*, *113*, D06115, doi:10.1029/JD2006007657.

Lee, J., J. Worden, D. Noone, K. Bowman, A. Eldering, A. LeGrande, J.-L. F. Li, G. Schmidt, and H. Sodemann (2011), Relating tropical ocean clouds to moist processes using water vapor isotope measurements, *Atmos. Chem. Phys.*, *11*, 741–752.

Lee, J.-E., and I. Fung (2008), Amount effect of water isotopes and quantitative analysis of post-condensation processes, *Hydrol. Processes*, *22*, 1–8.

Lin, Y.-L., R. D. Farley, and H. D. Orville (1983), Bulk parameterization of the snow field in a cloud model, *J. Climate Appl. Meteor.*, *22*, 1065–1092.

Majoube, M. (1971), Fractionnement en oxygène 18 et en deutérium entre l'eau et sa vapeur, *J. Chim. Phys.*, *68*, 1423–1436.

Mapes, B. E., and R. A. Houze (1995), Diabatic divergence profiles in Western Pacific mesoscale convective systems, *J. Atmos. Sci.*, *52*, 1807–1828.

Njitchoua, R., L. Sigha-Nkamdjou, L. Dever, C. Marlin, D. Sighomnou, and P. Nia (1999), Variations of the stable isotopic compositions of rainfall events from the Cameroon Rain Forest, Central Africa, *J. Hydrol.*, *223*, 17–26.

Raymond, D. J., and X. Zeng (2005), Modelling tropical atmospheric convection in the context of the weak temperature gradient approximation, *Q. J. R. Meteorol. Soc.*, *131*(608), 1301–1320.

- Risi, C., S. Bony, and F. Vimeux (2008a), Influence of convective processes on the isotopic composition ($\delta^{18}\text{O}$ and δD) of precipitation and water vapor in the tropics: 2. Physical interpretation of the amount effect, *J. Geophys. Res.*, *113*, D19305, doi:10.1029/2008JD009942.
- Risi, C., S. Bony, F. Vimeux, L. Descroix, B. Ibrahim, E. Lebreton, and B. Sultan (2008b), What controls the isotopic composition of the African Monsoon precipitation? Insights from event-based precipitation collected during the 2006 AMMA field campaign, *Geophys. Res. Lett.*, *35*, L24808, doi:10.1029/2008GL035920.
- Risi, C., S. Bony, F. Vimeux, M. Chong, and L. Descroix (2010), Evolution of the water stable isotopic composition of the rain sampled along Sahelian squall lines, *Q. J. R. Meteorolog. Soc.*, *136*(S1), 227–242.
- Rozanski, K., L. Araguas-Araguas, and R. Gonfiantini (1993), Isotopic patterns in modern global precipitation, in *Climate Change in Continental Isotopic Records*, *Geophys. Monogr. Ser.*, vol. 78, edited by P. K. Swart et al., pp. 1–36, AGU, Washington, D. C.
- Skamarock, W. C., and J. B. Klemp (2008), A time-split non-hydrostatic atmospheric model for weather research and forecasting applications, *J. Comput. Phys.*, *227*, 3465–3485.
- Sobel, A. H., and C. S. Bretherton (2000), Modeling tropical precipitation in a single column, *J. Clim.*, *13*(24), 4378–4392.
- Stewart, M. K. (1975), Stable isotope fractionation due to evaporation and isotopic exchange of falling waterdrops: Applications to atmospheric processes and evaporation of lakes, *J. Geophys. Res.*, *80*(9), 1133–146.
- Vuille, M., R. S. Bradley, M. Werner, R. Healy, and F. Keimig (2003), Modeling $\delta^{18}\text{O}$ in precipitation over the tropical Americas: 1. Interannual variability and climatic controls, *J. Geophys. Res.*, *108*(D6), 4174, doi:10.1029/2001JD002038.
- Yoshimura, K., T. Oki, N. Ohte, and S. Kanae (2003), A quantitative analysis of short-term ^{18}O variability with a Rayleigh-type isotope circulation model, *J. Geophys. Res.*, *108*(D20), 4647, doi:10.1029/2003JD003477.